Thermal conductivity and photoluminescence of light-emitting silicon nitride films

Amy Marconnet,[1,a)] Matt Panzer,[1,b)] Selçuk Yerci,[2,c)] Salvatore Minissale,[2] X. Wang,[4] X. Zhang,[4] Luca Dal Negro,[2,3] and K. E. Goodson[1]

[1]Department of Mechanical Engineering, Stanford University, 440 Escondido Mall, Building 530, Room 224, Stanford, California 94305, USA
[2]Department of Electrical and Computer Engineering & Photonics Center, Boston University, 8 Saint Mary's Street, Boston, Massachusetts 02215-2421, USA
[3]Division of Materials Science and Engineering, Boston University, Brookline, Massachusetts 02446, USA
[4]Department of Mechanical Engineering, Boston University, Boston, Massachusetts 02215, USA

Silicon-rich and rare-earth-doped nitride materials are promising candidates for silicon-compatible photonic sources. This work investigates the thermal conductivity and photoluminescence (PL) of light emitting samples fabricated with a range of excess silicon concentrations and annealing temperatures using time-domain picosecond thermoreflectance and time-resolved photoluminescence. A direct correlation between the thermal conductivity and photoluminescence dynamics is demonstrated, as well as a significant reduction of thermal conductivity upon incorporation of erbium ions. These findings highlight the role of annealing and stoichiometry control in the optimization of light emitting microstructures suitable for the demonstration of efficient Si-compatible light sources based on the silicon nitride platform. © 2012 American Institute of Physics. [doi:10.1063/1.3682508]

Amorphous silicon-rich silicon nitride films with various excess silicon concentrations (SiN_x) including those with additional erbium impurities ($Er:SiN_x$), are promising for light sources that are compatible with silicon-based electronics.[1–5] The $Er:SiN_x$ compound integrated with photonic crystal (PC) (Ref. 1) and plasmonic structures[6] shows an enhanced photoluminescence (PL) peak at 1.54 μm.[2,3] Moreover, $Er:SiN_x$-based light emitting devices operating at 1.54 μm have recently been demonstrated.[7] The structural, optical, and electrical properties of these materials have been extensively investigated.[1–3,5] Photonic crystal cavities fabricated from $Er:SiN_x$ with a stoichiometric silicon nitride matrix have been pumped to transparency, which is a step towards achieving on-chip laser sources.[1,8] However, to induce laser oscillations, it is crucial to predict and optimize the thermal behavior of the cavity as well. Device performance and stability can be improved by maximizing the thermal conductivity in order to prevent significant heating of the PC cavity. Because of the confined geometry of the proposed light sources, achieving a high thermal conductivity in the constituent materials is a dominant consideration in achieving targeted power densities. Nanostructural characteristics, such as the presence of bonding defects, are influenced by the processing conditions of the nitride films and impact the PL intensity and lifetime,[3] and these same characteristics can strongly influence thermal conduction.

This work measures the effect of processing parameters, specifically Si and Er concentrations and annealing tempera-

ture, on the thermal and optical properties of silicon-rich nitride films. Optimal processing conditions considering both thermal and optical properties are explored through a systematic study of the impact of annealing temperature and silicon concentration. The thermal properties of SiN_x samples with 7 different silicon concentrations (from 44.2 to 61.8% Si) and 6 annealing temperatures (T_{anneal} from 600 to 1100 °C), as well as those of the as-deposited films, are compared with the PL lifetime measurements of SiN_x samples. For the sample with a Si concentration of 50.0%, the impact of erbium doping on thermal conduction is investigated.

Amorphous SiN_x samples with different excess Si concentrations are fabricated by N_2 reactive magnetron co-sputtering using Si target. $Er:SiN_x$ films were fabricated at a constant Si concentration with varying Er concentrations. After deposition, the samples were annealed at temperatures between 600 and 1100 °C for 200 s under forming gas (5% H_2, 95% N_2) atmosphere. Details of sample preparation can be found in Ref. 2. The SiN_x films ($\sim$400 nm thick) investigated by time-resolved photoluminescence (TRPL) and time-domain thermoreflectance (TDTR) measurement are fabricated in the same batch, while the $Er:SiN_x$ films are $\sim$1300 nm thick and SiN_x samples analyzed by nanoindentation experiments are $\sim$1000 nm-thick. A JEOL 6100 scanning electron microscope (SEM) equipped with an energy dispersive x-ray (EDX) spectrometer (Oxford Instruments) was employed to quantitatively analyze the compositional content of the SiN_x and $Er:SiN_x$ films. Based on the result from a Monte Carlo simulation, a low electron beam voltage of 4 kV is selected for the EDX analysis to ensure that the interaction volume of the electron beam and specimen was confined within the 400 nm top layer SiN_x films. Nanoindentation is performed at room temperature using a Triboindenter nanomechanical testing system (Hysitron Inc., MN) with a

a)Author to whom correspondence should be addressed. Electronic mail: amymarco@stanford.edu.
b)Present address: KLA-Tencor Corporation, Milpitas, California 95035, USA.
c)Present address: Department of Mechanical Engineering, Massachusetts Institute of Technology, Cambridge, Massachusetts 02139, USA.

standard Berkovich tip. Both of the machine compliance and the tip area function were calibrated using a standard fused silica sample. Thermal drift is minimized by allowing thermal equilibrium to be reached inside the isothermal enclosure of the Triboindenter overnight preceding any indentation experiments. Constant loading rate control measuring scheme was chosen for Young's modulus and hardness characterization of SiN$_x$ thin film samples. Loading and unloading rates were kept at 900 μN/s. A maximum load of 4500 μN minimizes the effects from the substrate, which restrained the displacements (penetration into the thin films) to be within 10% to 15% of the total thin film thickness.

Picosecond TDTR is a well-established pump-probe technique for measuring the thermal conductivity and interface thermal resistances of thin films.[9–12] A metal transducer layer (35 nm of aluminum, deposited on the samples for TDTR) is heated by the frequency-doubled 532 nm, 20 mW, 10 μm diameter, 9.2 ps pump pulses from a mode-locked Nd:YVO$_4$ laser with a repetition rate of 82 MHz, modulated at 5 or 8 MHz for lock-in detection. The optically delayed 1064 nm, 5 mW, 5 μm diameter probe pulses derived from the same laser reflect off the metal surface and are detected by a fast photodetector to measure the surface temperature decay. Fitting the measured thermal decay trace to the solution of the radial-symmetric three-dimensional heat diffusion equation for the multilayer stack with surface heating by a modulated periodic pulse train allows extraction of the thermal conductivity and interface resistances within the sample structure.

To resolve the effective PL lifetime, τ_{PL}, the samples are excited by the second harmonic of the Mai Tai laser at 430 nm with 100 fs pulses. The TRPL signal is dispersed through a double grating spectrometer (Acton Spectra Pro. 2300i) and detected using a single-photon counting streak camera with 10 ps time-resolution (Hamamatsu, C4770). For all the samples, the PL decay trace are fitted by a two-exponential decay model. In order to compare the lifetime data of different samples, we have defined an effective PL lifetime as $\tau_{PL} = (A_1 \times \tau_1 + A_2 \times \tau_2)/(A_1 + A_2)$. This choice is due to the strongly non-exponential nature of the time evolution of SiN$_x$ PL.[3]

Measurements of time-dependent PL and picosecond time-domain thermoreflectance of identical samples allow for direct comparison of the effect of the excess silicon in SiN$_x$ and post-annealing temperature on both PL lifetime and thermal conductivity. The thermal conductivity of all samples ranges from 1.25 to 2.66 W m^{-1} K^{-1} (as shown in Figure 1(a)), while the thermal boundary resistance between the SiN$_x$ layer and the metal transducer layer ranges from 3.1 to 6.5 m^2 K GW^{-1} (not shown). The effective PL of SiN$_x$ samples ranges from 0.1 ns to 1.0 ns (as shown in Figure 1(b)). Samples with silicon concentration greater than 53% did not show enough PL intensity to measure the lifetime. High thermal conductivity and long PL lifetime are observed at low excess silicon concentrations and high annealing temperatures. PL lifetime (τ_{PL}) depends on both radiative and non-radiative mechanisms, $\tau_{PL}^{-1} = \tau_r^{-1} + \tau_{nr}^{-1}$, where τ_r and τ_{nr} are radiative and non-radiative PL lifetimes, respectively. The PL lifetime of SiN$_x$ is dominated by non-radiative interactions which are primarily driven by relaxations at
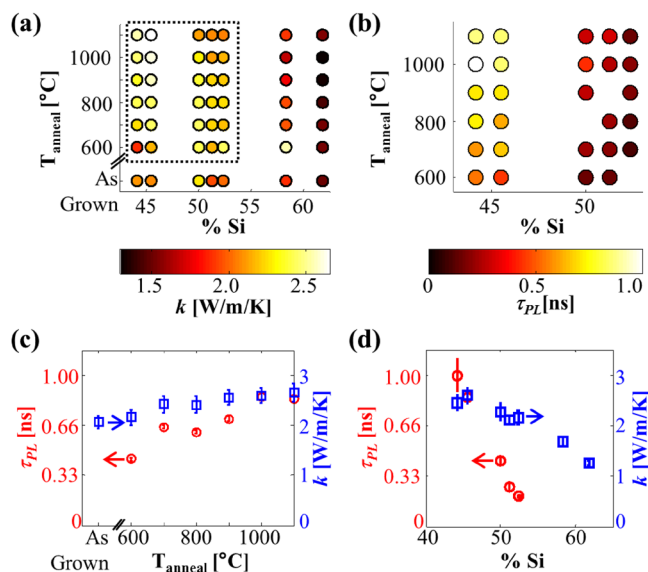

FIG. 1. (Color online) Impact of annealing temperature and silicon concentration on (a) thermal conductivity, k, and (b) effective PL lifetime, τ_{PL}. (c) Correlation of the trend of increasing thermal conductivity (squares) and PL lifetime (circles) with anneal temperature for samples with a relative Si concentration of 45.5%. (d) Correlation of the trend of decreasing thermal conductivity (squares) and PL lifetime (circles) with increasing excess silicon concentration for samples annealed at 1000 °C.

impurity-induced and disorder-induced defect sites. To highlight the trends in thermal conductivity and PL lifetime, Figure 1(c) shows the increasing thermal conductivity and PL lifetime with increasing annealing temperature for one value of excess Si concentration (45.5%), and Figure 1(d) shows the increasing thermal conductivity and PL lifetime with decreasing silicon concentration for one annealing temperature (1000 °C).

The thermal conductivity of the SiN$_x$ films can be very roughly approximated as $k = \frac{1}{3} c v^2 \tau_{ph}$, where c is the volumetric heat capacity, v is the acoustic velocity of the phonons, and τ_{ph} is the relaxation time of the phonons. While the use of phonon transport theory for this highly disordered material is questionable, this approach serves here to provide an approximate scaling of the trends of thermal conductivity with acoustic velocity and other properties. The heat capacity is approximately constant with stoichiometry and annealing temperature, and can be approximated as $c \sim n_a k_b$, where n_a is the atomic density and k_b is Boltzmann constant. Combined Rutherford backscattering and spectroscopic ellipsometry measurements (of Er:SiN$_x$ samples) indicate no statistically significant change in the atomic density of the samples with increasing silicon concentration or annealing temperature, but the density, ρ, increases with the incorporation of heavier silicon atoms. Nanoindentation measurements shows that the elastic modulus, E, of the films decreases with increasing silicon concentration (as shown in Figure 2(a)). The acoustic velocity of phonons in the film ($v \sim \sqrt{E/\rho}$) decreases with increasing silicon concentration, since the elastic modulus decreases while the density of the films increases. Figure 2(b) shows a comparison of the measured thermal conductivity and the predicted trends in thermal conductivity from this model assuming a constant phonon lifetime. The acoustic velocity is estimated using the best fit
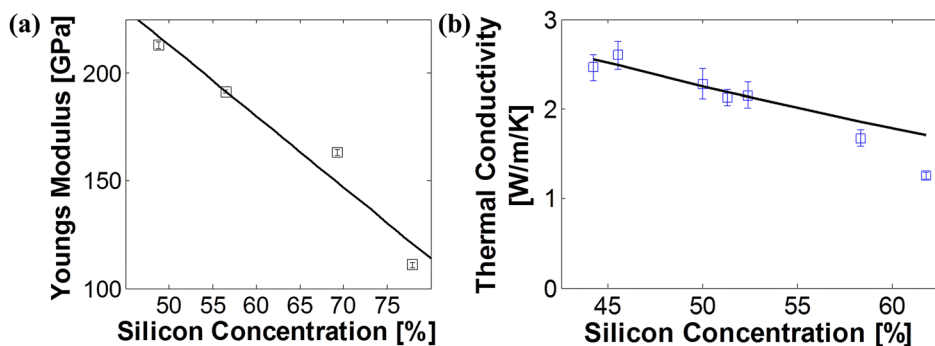
FIG. 2. (Color online) (a) Impact of silicon concentration on Young's modulus and hardness of amorphous SiN_x films. The straight line is a best fit to the data and serves mainly as a guide for the reader. (b) SiN_x thermal conductivity as a function of silicon concentration for samples annealed at 1000 °C. The solid line shows the predicted trend in thermal conductivity using the measured elastic modulus (best-fit line from (a)) in the calculation of acoustic velocity, and a constant phonon lifetime estimated from a best fit to the data with relative Si concentration <55%.

line to the elastic modulus data (as shown in Figure 2(a)) and the mass density calculated from the measured atomic density and silicon concentrations combined and the atomic masses of silicon and nitrogen. At the highest silicon concentrations, the thermal conductivity falls below the predicted value for a constant τ_{ph} indicating that in addition to reduction in acoustic velocity, the phonon lifetime also decreases with increasing silicon concentration. The phonon mean free path, $\lambda_{ph} = v\tau_{ph}$, decreases with increasing silicon concentration. The dominant sources of phonon scattering are disorder and defects, both of which may be impacted by annealing temperature and silicon concentration. The reduced phonon mean free path with increasing silicon concentration suggests a higher concentration of defects and/or disorder in the films with high silicon concentrations. The corresponding reduction in PL lifetime (Figure 1(d)), also impacted by disorder and defects, agrees well with the thermal results.

The interplay between disorder and defect concentration could also account for the trends in thermal conductivity with annealing temperature. At low excess silicon concentrations, the thermal conductivity increases with annealing temperature. Increasing annealing temperature reduces disorder and passivates bond defects, and therefore the phonon relaxation time, thermal conductivity, and the effective PL lifetime are enhanced. At high silicon concentrations, the thermal conductivity is approximately constant with annealing temperature. The increased defect concentration related to the high excess silicon concentration may dominate over the slight reduction in disorder. At intermediate silicon con-

centrations (about 50% Si), a peak in the thermal conductivity is observed at annealing temperatures lower than the maximum annealing temperature, which may be due to the interplay between intrinsic defects and thermally induced defects such as those formed at the nanoinclusion interfaces.[2]

Doping SiN_x films with erbium[2,3] leads to strong PL at 1.54 μm which is significant for photonic applications.[2,3] In the previous studies of similarly fabricated erbium-doped SiN_x films, the Er PL lifetime at 1.54 μm, related to the PL efficiency, was maximized at low silicon concentrations and high anneal temperatures,[3] similar to the behavior for undoped films reported here. However, doping with erbium forms another scattering mechanism impeding thermal transport and reduces the thermal conductivity. The effective PL lifetime of SiN_x also decreases due to energy transfer from SiN_x to Er ions at relatively low Er concentrations ($\sim 4 \times 10^{20}$ cm^{-3}).[2,3] Figure 3 shows the thermal conductivity of erbium doped silicon nitride films (50% silicon) annealed at 1000 °C. At an erbium concentration of 3.2×10^{21} cm^{-3}, the thermal conductivity was reduced to 1.5 W/m/K, less than 65% of the undoped SiN_x value (2.3 W/m/K). It is well-known that large ions act as scattering centers for phonons and therefore erbium incorporation decreases the thermal conductivity. It should also be noted that Si concentration of SiN_x decreases slightly with Er concentration which should have slightly increased the thermal conductivity.

In conclusion, both thermal and optical properties of silicon nitride films (SiN_x) and Er-doped SiN_x depend on the post-annealing temperature, the amount of excess silicon, and erbium incorporation. The maximum thermal conductivity and longest PL lifetime were observed at low excess silicon concentrations and high annealing temperatures. We demonstrate that SiN_x thermal conductivity decreases due to reduced acoustic velocity and increased scattering of phonons, while its effective PL lifetime shortens as a result of non-radiative recombinations at defect-induced states in SiN_x. Thermal conductivity of Er:SiN_x matrix decreases with excess Er concentrations. The overlap of ideal processing conditions for both thermal and optical performance is advantageous for SiN_x and Er:SiN_x photonic crystal devices[1] and should be considered when fabricating devices to ensure the very best optical performance, while efficiently removing heat from the device regions.
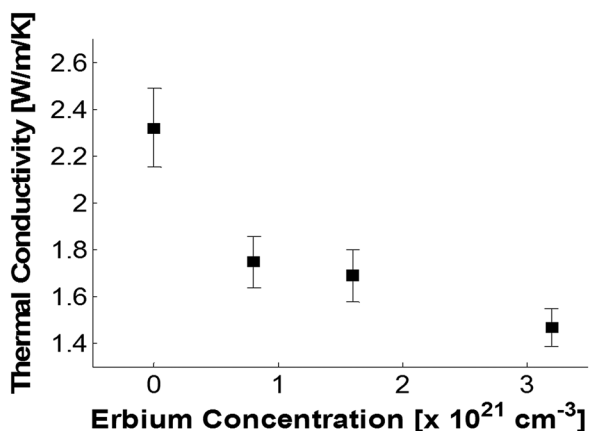

FIG. 3. Impact of erbium concentration on the thermal conductivity of an Er-doped silicon-rich nitride film with a relative Si concentration of 50%.

[1]Y. Gong, M. Makarova, S. Yerci, R. Li, M. Stevens, B. Baek, S. W. Nam, L. Dal Negro, and J. Vuckovic, Opt. Express **18**(13), 13863 (2010).

[2]S. Yerci, R. Li, S. O. Kucheyev, T. van Buuren, S. N. Basu, and L. Dal Negro, Appl. Phys. Lett. **95**(3), 031107 (2009).

[3]S. Yerci, L. Rui, S. O. Kucheyev, T. van Buuren, S. N. Basu, and L. Dal Negro, IEEE J. Sel. Top. Quantum Electron. **16**(1), 114 (2010).

[4]Z. H. Cen, T. P. Chen, L. Ding, J. D. Ye, Y. Liu, M. Yang, J. I. Wong, Z. Liu, and S. Fung, Electrochem. Solid-State Lett. **12**(2), H38 (2009).

[5]R. Li, J. R. Schneck, J. Warga, L. D. Ziegler, and L. Dal Negro, Appl. Phys. Lett. **93**(9), 091119 (2008).

[6]A. Gopinath, S. V. Boriskina, S. Yerci, R. Li, and L. Dal Negro, Appl. Phys. Lett. **96**(7), 071113 (2010).

[7]S. Yerci, R. Li, and L. Dal Negro, Appl. Phys. Lett. **97**(8), 081109 (2010).

[8]A. C. Hryciw, R. D. Kekatpure, S. Yerci, L. Dal Negro, and M. L. Brongersma, Appl. Phys. Lett. **98**(4), 041102 (2011).

[9]D. G. Cahill, Rev. Sci. Instrum. **75**(12), 5119 (2004).

[10]A. Schmidt, M. Chiesa, X. Chen, and G. Chen, Rev. Sci. Instrum. **79**(6), 064902 (2008).

[11]M. A. Panzer, M. Shandalov, J. A. Rowlette, Y. Oshima, C. Yi Wei, P. C. McIntyre, and K. E. Goodson, IEEE Electron Device Lett. **30**(12), 1269 (2009).

[12]J. P. Reifenberg, C. Kuo-Wei, M. A. Panzer, K. Sangbum, J. A. Rowlette, M. Asheghi, H. S. P. Wong, and K. E. Goodson, IEEE Electron Device Lett. **31**(1), 56 (2010).